Cyclic Pore Pressure Generation in Silty Soils under the Action of Combined Waves and Current

Yi-Fa Wang[1], Fu-Ping Gao[2]*, and Wen-Gang Qi[3]
[1,2,3]*Key Laboratory for Mechanics in Fluid Solid Coupling Systems, Institute of Mechanics, Chinese Academy of Sciences, Beijing, China*
**E-mail*: fpgao@imech.ac.cn

ABSTRACT: Ocean waves and current always coexist in the offshore shallow water environments, which may bring the corresponding seabed responses more complex than those under pure waves. The responses of a silty soil under the action of combined waves and current were physically modeled with a specially designed water flume. A series of tests for the progressive waves with a following-current or with an opposing-current have been conducted, respectively. Both the water-surface elevation and the pore pressure, including the transient and residual components, at various depths in the silty soil were measured simultaneously. The effects of both wave loading history and superimposing current upon waves on the pore pressure responses are examined. It is indicated that the amplitude of the transient pore-pressure component is enlarged for the following-current case and reduced for the opposing-current case. The maximum amplitude of the residual pore-pressure component decreases gradually during the subsequent series of wave loading under the same wave conditions.

KEYWORDS: Pore pressure responses, Silty soil, Combined waves and current, Physical modeling

1. INTRODUCTION

While the ocean waves are propagating over the seabed in the shallow waters, the pore-pressure could be generated in the sediments. Two mechanisms of the pore pressure responses have been observed: one is the oscillatory or transient pore pressure accompanied by the decrease of amplitude and phase lag in the pore pressure; the other is the progressive buildup of pore pressure or residual pore pressure caused by the cyclic shear stress variation (e.g. Seed & Rahman, 1978; McDougal *et al.*, 1989; Sassa & Sekiguchi, 1999; Sumer *et al.*, 1999; Jeng *et al.*, 2007). When the effective stresses between the individual grains vanish because of the pore-pressure buildup, soil liquefaction occurs and the sediment mixture acts like a fluid. Liquefaction may induce the instability of seabed and is thereby a potential threat to offshore structures.

Numerous studies have been devoted to the theoretical and experimental investigations of the transient and residual pore-pressure responses of the seabed under the action of waves. Yamamoto *et al.* (1978) and Madsen (1978) derived analytical solutions of wave-induced changes in stresses and displacements in semi-infinite porous media based on Biot's consolidation theory (1941), respectively. Seed & Rahman (1978) first proposed a model to describe the buildup of pore pressure under progressive waves. The buildup of residual pore-pressures in silty soils was observed in water flume tests by a few researchers, e.g. Clukey *et al.* (1985), Foda & Tzang (1994). Sassa & Sekiguchi (1999) investigated the behavior of sand bed with d_{50} = 0.15mm under progressive and standing waves in a centrifuge wave tank. Their results showed that soil liquefaction occurs due to the buildup of pore pressure and the liquefaction front advances downward. Meanwhile, re-liquefaction is more difficult to occur at deeper soil locations as the soil there gets more densified. Miyamoto *et al.* (2004) proposed a theoretical model to describe the process of solidification in liquefied sands and also to predict the progressive liquefaction. The densification associated with solidification was further examined. Sumer *et al.* (2006) conducted a series of experiments focusing on the sequence of sediment behavior during wave-induced liquefaction including the buildup of pore pressure, liquefaction and compaction of the sediment.

The aforementioned studies primarily focused on the sandy or silty soils subjected to pure wave loading, while little attention has been paid to the dynamic responses of a soil under the action of combined waves and current. In the offshore environments, the ocean waves are always coupled with current, which brings the seabed responses more complex than those under pure waves. The wave-induced pore-pressure responses of seabed could be influenced by imposing a current (Zhang *et al.*, 2013; Qi & Gao, 2014). However, the experimental investigation on the seabed responses under combined waves and current is quite scarce up to now, and effects of current on the seabed responses are far from understanding.

In the present study, a series of experiments with either the following current or the opposing current superimposed on the waves, were conducted in a specially designed water flume. The transient and residual pore pressures at various depths in the silty bed were measured with miniature pore pressure transducers. Based on the experimental results, the effects of both wave loading history and superimposing current upon waves on the pore-pressure responses are investigated.

2. EXPERIMENTAL DESIGNS

2.1 Experimental Set-up

The experiments were conducted in a fluid-structure-soil interaction flume (52.0 m long, 1.0m wide and 1.5m high) at the Institute of Mechanics, Chinese Academy of Sciences. This specially designed flume is capable of synchronously generating waves and current. Waves can be generated with a piston-type wave generator located at the upstream of the flume; Meanwhile, a porous plastic-net type sloped wave absorber are employed at the downstream end to efficiently eliminate wave reflection. As illustrated in Figure 1, a large soil box (6.0m in length, 1.0m in width and 1.8m in depth) is located in the middle section of the flume, and a segment of 4.0m×1.0m×0.6m (length × width × depth) with edges flush with the bottom of the flume was employed in this series of experiments. The water depth (h) in the flume was maintained at 0.6m for all tests.

In the experiments, 14 miniature pore pressure transducers (PPTs) were utilized to measure the wave-induced cyclic pore-pressure in the silt. The arrangement of the PPTs is detailed with filled circles in Fig. 1. Four wave height gauges were located just above the PPTs. An Acoustic Doppler Velocimetry (ADV) was installed to measure the flow velocity at the level of 0.5h (i.e. 0.3m) above the soil surface at the central line of the soil box.

The signals of wave height gauges and pore pressure transducers were synchronously sampled via the NI USB-6255 Data Acquisition Card. The sampling frequency for the measurements was 100 Hz.

2.2 Preparation of a Dense Silty Soil: Soil Properties

Before test silt is deposited into the soil box, the 14 PPTs were installed at the designated locations with the support of vertical racks (see Figure 1). After that, the soil box was partially filled with water for the de-airing purpose. Then, the dry silt particles were sprayed into the water gently to avoid air bubbles mixed into the sediment. The slurry of test silt was gradually made with increasing the water level and meanwhile spraying grains step by step. This process was continued until the surface of test silt got flush with the flume bottom. The silty soil was left to consolidate in water for two weeks to achieve a dense state before the wave loading tests.

The grain size distribution of the test silt is shown in Figure 2. The main properties are summarized in Table 1. It is noted that the coefficient of permeability k_s, is determined from $k_s = 3500 d_{10}^{1.65}$ in units of gallons per day per square foot, i.e. GPD/FT^2 (Shepherd, 1989). The coefficient K_0, the ratio between horizontal and vertical effective stresses, is determined from $K_0 = 1 - \sin\varphi$ (Lambe & Whitman, 1969) in which φ is the internal friction angle.

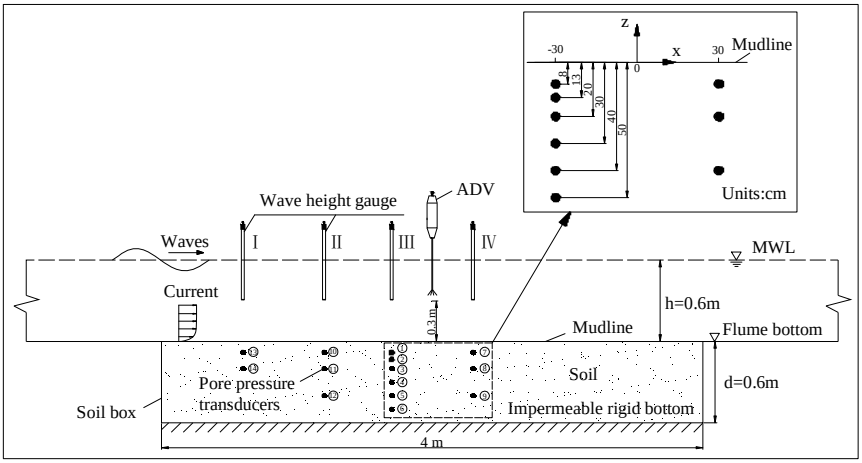

Figure 1 Schematic diagram of the experimental system

Table 1 Properties of test silt

Mean size of silt grains	Geometric standard deviation	Internal friction angle	Ratio of horizontal and vertical effective stresses	Coefficient of permeability	Plasticity index	Initial void ratio	Relative density	Submerged unit weight of soil
d_{50} (mm)	$\sigma_g = \frac{d_{84}}{d_{50}}$	ϕ (°)	K_0	k_s (m/s)	I_p (%)	e_0	D_r	γ' (kN/m^3)
0.047	1.62	26.3	0.56	7.54×10^{-7}	7.6	0.41	0.85	11.47

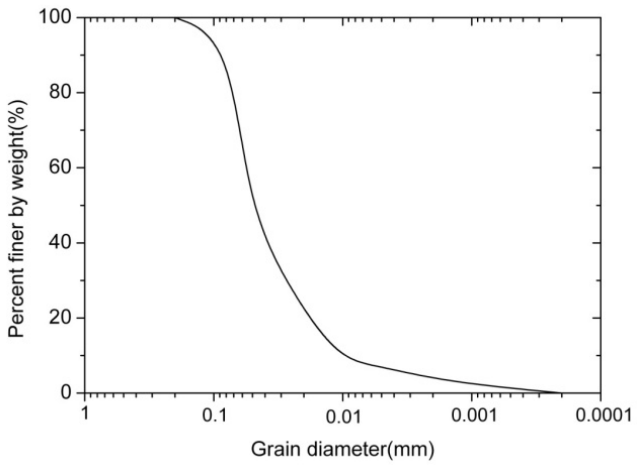

Figure 2 Grain size distribution curves of the test silt

2.3 Test Conditions

Test conditions are summarized in Table 2. The water depth (h) was kept constant at 0.6 m. Regular waves were adopted to conveniently analyze the pore pressure responses and orbital velocities of the flow. The quantity H in the table is the wave height, T the wave period. The quantities U_c and U_{wm} are individually the velocity of the current component and the amplitude of wave orbital velocity, measured at the level of 0.5h above the soil-bed. U_m is the maximum value of combined wave and current velocity at the same level of U_c and U_{wm}. In Table 2, U_c = 0 represents the conditions of waves alone, while the positive value of U_c represents the conditions of waves plus a following current and the negative value of U_c represents the conditions of waves plus an opposing current.

The other series of experiments were carried out to investigate the effects of wave loading history on the pore water pressure responses. Four stages of wave loading were measured and fixed wave conditions were adopted (i.e. H = 7 cm, T = 1.5 s). Note that the duration of wave generation was more than 20 min and the subsequent waves were switched on after all the excess pore pressure had dissipated due to the previous wave loading.

Table 2 Summary of experimental conditions

Test	H (m)	T (s)	U_c (m/s)	U_{wm} (m/s)	U_m (m/s)
1-1	0.118		0		0.101
1-2	0.112		0.11		0.214
1-3	0.127	1.2	-0.11	0.101	0.007
1-4	0.106		0.20		0.294
1-5	0.133		-0.20		-0.112
2-1	0.115		0		0.158
2-2	0.105		0.11		0.260
2-3	0.120	1.4	-0.11	0.158	0.049
2-4	0.098		0.20		0.333
2-5	0.139		-0.20		-0.052
3-1	0.111		0		0.160
3-2	0.099		0.11		0.250
3-3	0.112	1.6	-0.11	0.160	0.032
3-4	0.082		0.20		0.327
3-5	0.119		-0.20		-0.065
4-1	0.111		0		0.184
4-2	0.105		0.11		0.279
4-3	0.118	1.8	-0.11	0.184	0.075
4-4	0.086		0.20		0.352
4-5	0.122		-0.20		-0.006
5-1	0.097		0		0.168
5-2	0.095		0.11		0.265
5-3	0.105	2.0	-0.11	0.168	0.059
5-4	0.083		0.20		0.369
5-5	0.122		-0.20		0.000

2.4 Testing Procedure

The testing procedure was adopted as follows:

(1) Empty and clean the flume including the soil box. Prepare the PPTs and test silt as stated in Section 2.2.
(2) Fill up the flume gradually with water to a given depth of 0.6m.
(3) Switch on waves or waves with current together and sample the water surface elevation, the pore pressure and the flow velocity synchronously.
(4) Switch off waves or current and wait until the suspended sediment settles.
(5) Start next test when the pore pressure during the previous test dissipate completely.

3. RESULTS AND DISCUSSION

3.1 Effects of Wave Loading History on Pore Pressure Responses

When an initially loosely deposited silty bed is subjected to progressive waves, the excess pore pressure in the soil fluctuates while the mean value gradually builds up to a maximum value (p_{max}). This behavior of the silty bed has been reported in many previous flume studies (e.g. Foda & Tzang, 1994; Sumer *et al.*, 2006).

Figure 3 gives the time series of excess pore pressure for different stages of wave loading at z = -50 cm. The loading programme consisted of four series of wave loading stages. The pore pressure was measured in a relatively loosely deposited silt in the first stage of wave loading, and in a wave pre-loaded silt in the subsequent wave loading. For each stage of wave loading under the same wave conditions, the maximum accumulated pore pressure (p_{max}) decreases considerably with increasing the times of wave loading. It is indicated that in the fourth stage of wave loading, the pressure p_{max} was virtually nil. It could be explained by the fact that when the soil was subjected to wave loading, the soil grains rearranged through the buildup and dissipation process of the pore pressure. The silty soil gets consolidated and densified due to the previous wave loading, the soil becomes denser and hence the pore pressure is much harder to accumulate and therefore re-liquefaction is more difficult to occur.

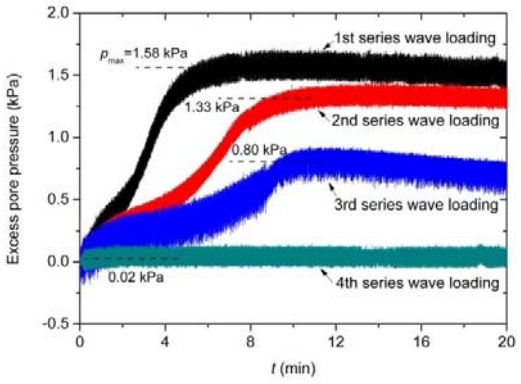

Figure 3 Time series of excess pore pressure for different stages of wave loading at z = -50cm (H = 7cm, T = 1.5s)

To describe the re-liquefaction mechanism, a non-dimensional parameter termed as liquefaction index (I_L) can be defined as

$$I_L = p_{max} \Big/ (-\frac{1+2K_0}{3}\gamma' z) \quad (1)$$

where I_L is the ratio of the maximum accumulated pore pressure and the initial mean effective stress considering the lateral earth pressure. No excess pore pressure is generated for the condition $I_L = 0$, while the residual liquefaction may occur for the condition I_L reaches the value of 1, which causes the vanishing of effective stresses and the total load will be carried by water alone, therefore the soil loses its strength. Thus I_L can be applied to assess the degree of soil stability under wave loading. With the properties of test silt listed in Table 1, the calculated value of I_L is about 39% in the first stage of wave loading at z = -50cm, much less than 1, which indicates that there is no liquefaction occurred at this depth. The magnitude of I_L becomes virtually negligible in the fourth stage of wave loading. It should be noted herein that there was no residual liquefaction occurred in the present series of experiments, since the relative density of the silty soil was relatively large (i.e. D_r = 0.85). Therefore, it is convenient to investigate the transient component of the pore pressure responses in the silty soil.

3.2 Effects of Wave Characteristics on Pore Pressure Responses

The vertical distributions of the wave-induced seabed responses versus soil depth under waves alone condition with various wave periods are given in Figure 4. The value of wave height is fixed at 11.0cm. The pore pressure responses scale up as the wave period increases. The distribution profiles of seabed responses with relatively short wave periods are somehow different from those with longer wave periods. The pore pressure gradients at the upper seabed reduce as the wave periods increase.

As illustrated in Figure 4, the depth profiles of the pore pressure amplitudes in silty bed are much more complex than the theoretical results developed by Yamamoto *et al.* (1978) and Madsen (1978) based on Biot's theory (1941), which indicated that amplitudes of oscillatory pore pressure in sandy soil tend to decrease deeper into the seabed. In the present experiments, the maximum amplitudes of the wave-induced pore pressure decrease rapidly near the seabed surface, while it is noted that there is a great increase of pore pressure near the rigid seabed bottom. This might be explained by the fact that the energy is reflected from the impermeable bottom of the soil box.

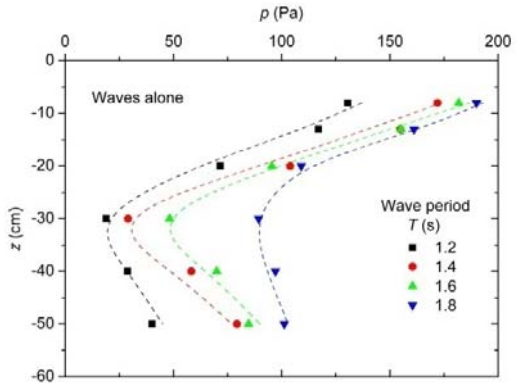

Figure 4 Comparison of depth profiles of the pore pressure amplitudes under waves alone condition between different value of wave periods (H = 11.0cm)

Figure 5 gives close-up picture of the excess pore pressure in the Test 3-1 at six given depths of the same section (PPTs 1 to 6 in Figure 1) under waves alone condition. Note that t is not the actual sampling time. t_{lag} denotes the time difference between various depth when the measured pore pressure gets peak value at z = -8cm. It is indicated that the regular wave-induced transient pore pressure presents a sinusoidal variation. The amplitudes of the oscillatory pore pressure show the similar trends with depth as aforementioned. As shown in Figure 5, there is a larger and larger phase lag in the pressure with increasing depth. Though not shown here, superimposing current upon waves scarcely has effects on the phase lag of the pore pressure responses.

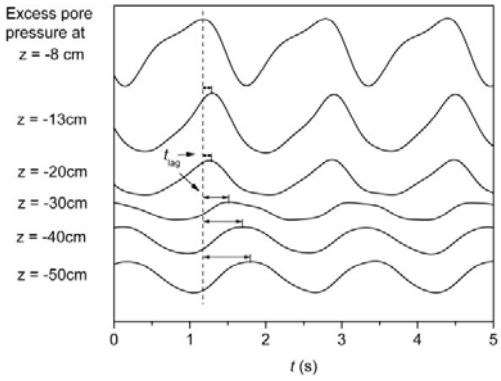

Figure 5 Close-up picture of the excess pore pressure at various depth in the silty bed under waves alone condition from Test 3-1

3.3 Effects of Superimposing a Current upon Waves on Pore Pressure Responses

A series of experiments listed in Table 2 were conducted to investigate the effects of current on the wave-induced seabed pore pressure responses when the accumulated excess pore pressure was relatively small comparing with the overburden pressure. It was demonstrated by Tzang (1998) that the relatively small buildup of mean pore pressure had insignificant effects on the unfluidized silt responses.

When a current is superimposed upon the progressive waves, the flow velocities are significantly changed and there exists nonlinear interactions between waves and current. In order to clearly show the nonlinear interaction effects, the flow velocities measured at the level of 0.5h above the soil-bed of tests 4-1, 4-4 and 4-5, are plotted in Figure 6. The flow velocities are averaged by phase and the sum of velocities under waves alone and current alone (following or opposing) are also depicted in Figure 6. It is indicated that the linear superposition of waves alone and current alone velocities is distinctly different from the actual velocity profiles under combined waves and current. The value of U_m is smaller than the sum of U_c and U_{wm} for the following-current case, while the value of U_m is larger than the sum of U_c and U_{wm} for the opposing-current case. This nonlinear interaction between waves and the current further affects the pore pressure responses.

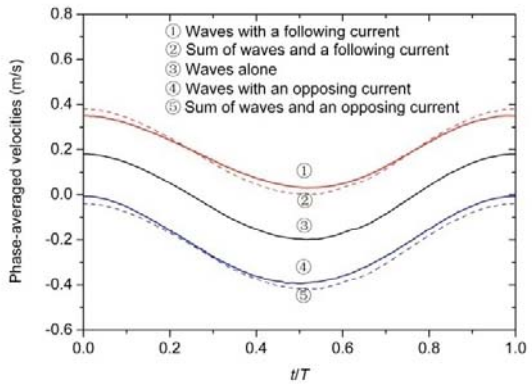

Figure 6 Comparison of flow velocity variation over one cycle between measured results (phase-averaged) and a sum of separately measured unidirectional current (U_c = 0.2m/s) and waves (H_0 = 11.1cm, T = 1.8s) at the level of 0.5h

Typical time series of pore pressure responses at the same measurement section of the flume with PPTs 2, 3 and 6 in the silty seabed are shown in Figure 7 from tests 3-1, 3-4 and 3-5 under conditions of waves alone, waves with a following current and waves with an opposing current. The wave height under waves alone is 11.1cm, while the wave height decreased to 8.2cm for the following-current case and increased to 11.9cm for the opposing-current case. The wave period is 1.6s. The flow velocities under current alone are ±0.20m/s. It is indicated that the excess pore pressure are oscillating with the wave load, and at the same time the mean value slightly builds up and asymptotically attains a maximum value in a short period. The value of I_L was less than 10%.

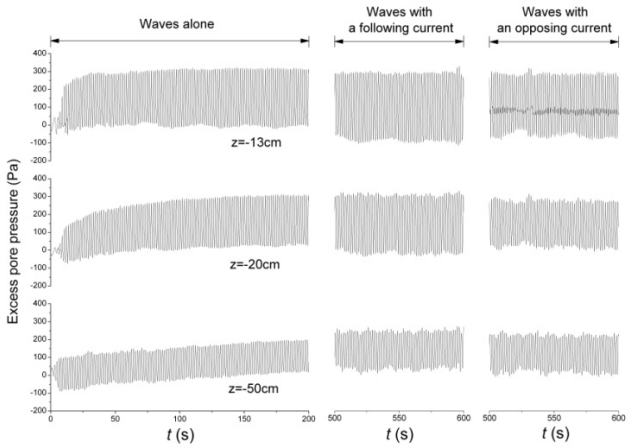

Figure 7 Typical time series of pore pressure responses at various depth in the silty bed under conditions of waves alone, waves with a following current and waves with an opposing current from Test 3-1, 3-4 and 3-5 (H_0 = 11.1cm, T = 1.6s, U_c = ±0.20m/s)

Figure 7 illustrates details of the amplitudes of oscillatory pore pressure differences at various depths under conditions of waves alone, waves with a following current and waves with an opposing current. The amplitudes of oscillatory pore pressure of the following-current case are basically greater than those of waves alone condition, while an opposite trend is observed in the opposing-current case. The amplitudes of the pore pressure responses strongly depend on the dynamic wave pressure acting on the surface of the soil-bed. It is evident that the higher wave height and the longer wave length, the larger the amplitude of the corresponding wave pressure on the soil-bed. The presence of a current in a propagating wave will change the wave characteristics. For instance, the following current will elongate the wave length and decrease the wave height, whereas these two changes exert opposite effects on the wave pressure acting on the surface of the soil-bed. The experimental results show that the amplitudes of the pore pressure for the following-current case are larger than the opposing-current case, which indicates that the change of wave length induced by superimposing a current upon waves plays a more important role in determining the transient pore pressure responses. It is of interest to mention that the time development of the mudline was not measured during the experimental procedure. As stated earlier, the silty soil was subjected to plenty of wave loading cycles and the relative density reached a relatively large value (larger than 0.9). The silty bed densified to a large degree and the settlement of the soil surface was so small that could be neglected. Also, the sediment transport was not expected to play a major role in the wave-induced pore pressure responses due to the short operating duration during which the waves and current had been switched on. Figure 8 gives the depth profile of amplitudes of oscillatory pore pressure in the silty bed under different combinations of waves and current loading from tests 1-1, 1-4 and 1-5. It shows the aforementioned trends under combined waves and current clearly, which are consistent with the experimental results on a sandy bed with d_{50} = 0.38mm by Qi & Gao (2014). The influence of introducing a current in waves is particularly significant in the region near the seabed surface where liquefaction commonly occurs (see Figure 8). The results imply that the momentary liquefaction is more likely to occur for the case of waves with a following current in contrast with waves alone condition.

It is also observed from Figure 8 that the relative differences of the amplitudes of the seabed responses under waves and following-current are unequal to those under waves and opposing-current when the magnitude of the current is same (i.e. U_c = 0.2m/s and U_c = -0.2m/s). This should be attributed to the nonlinear interactions between waves and current concerning the direction of current superimposed upon waves as aforementioned. The direction of current superimposed upon waves should be taken into account in predicting the pore pressure responses under the action of combined waves and current.

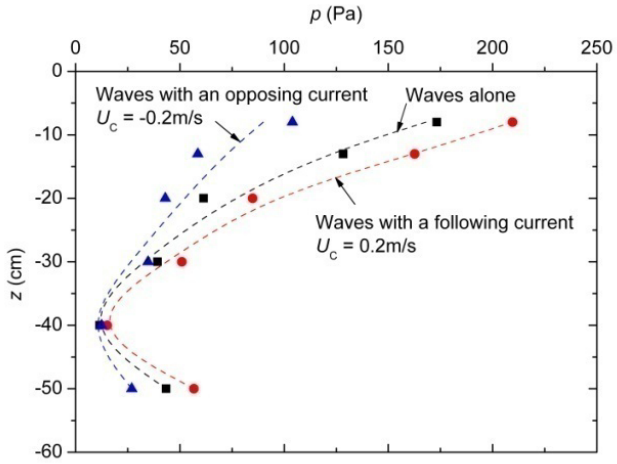

Figure 8 Comparison of depth profiles of the pore pressure amplitudes between the cases of waves alone, waves with a following current and waves with an opposing current (H_0 = 11.8cm, T = 1.2s)

4. CONCLUSIONS

In this study, the silt responses under regular waves and combined waves and current conditions were investigated by a series of experiments in a large fluid-structure-soil interaction flume. Based on the experimental results, the following conclusions are drawn:

(1) In the silty bed, the accumulated maximum pore pressure reduces considerably with the subsequent wave loading under the same wave conditions, as the soil bed being densified due to the grain rearrange in the process of buildup and dissipation of the pore pressure. Thus in the practical situations, the pore pressure may build up slightly when subjected to usual wave loading. The suggested non-dimensional parameter I_L can be applied to assess the degree of residual liquefaction and soil stability under wave loading.

(2) The depth profiles of the wave-induced pore pressure amplitudes in the silty bed show some different trends with the poro-elasticity theory, which is attributed to the finite thickness of the soil depth. The pore pressure responses increase as the wave period increases, while the pore pressure gradients at the upper seabed reduce as the wave periods increase.

(3) The amplitudes of oscillatory pore pressure under waves with a following current are basically greater than waves alone, while the amplitudes of oscillatory pore pressure under waves with an opposing current are smaller than waves alone. Superimposing a following current upon waves brings the momentary liquefaction easier to occur in a silty soil.

5. ACKNOWLEDGEMENTS

This work is financially supported by the Major State Basic Research Development Program of China (973 Program) (Grant No. 2014CB046204) and National Natural Science Foundation of China (Grant No. 11232012).Technical assistance in the flume experiments from Assistant Professor Cun Hu, Mr. Ning Wang, and Mr. Haiyang Jiang is greatly appreciated.

6. REFERENCES

Biot, M.A. (1941). "General theory of three-dimensional consolidation". Journal of Applied Physics 12 (2), pp155–164.

Clukey, E.C., Kulhawy, F.H. and Liu, P.L.F. (1985). "Response of silts to wave loads: experimental study". Strength testing of marine sediments, laboratory and in-situ measurements, ASTM STP, 883, pp381-396.

Foda, M.A. and Tzang, S.Y. (1994). "Resonant fluidization of silty soil by water waves". Journal of Geophysical Research 99 (C10), pp20463–20475.

Jeng, D.S., Seymour, B., Gao, F.P. and Wu, Y.X. (2007). "Ocean waves propagating over a porous seabed: Residual and oscillatory mechanisms". Science in China Series E: Technological Sciences 50(1), pp81–89.

Lambe, T.W. and Whitman, R.V. (1969). "Soil Mechanics". John Wiley and Sons, Inc., New York.

Madsen, O.S. (1978). "Wave-induced pore pressures and effective stresses in a porous bed". Geotechnique 28 (4), pp377–393.

McDougal, W.G., Liu, P.L.F., Clukey, E.C. and Tsai, Y.T. (1989). "Wave-induced pore water pressure accumulation in marine soils". Journal of Offshore Mechanics and Arctic Engineering 111(1), pp1-11.

Miyamoto, J., Sassa, S. and Sekiguchi, H. (2004). "Progressive solidification of a liquefied sand layer during continued wave loading". Geotechnique 54(10), pp617-629.

Qi, W.G., Gao, F.P. (2014). "Water flume modeling of dynamic responses of sandy seabed under the action of combined waves and current: Turbulent boundary layer and pore-water pressure". 8th International Conference on Physical Modelling in Geotechnics 2014, pp561-567.

Sassa, S. and Sekiguchi, H. (1999). "Wave-induced liquefaction of beds of sand in a centrifuge". Geotechnique 49(5), pp621–638.

Seed, H.B. and Rahman, M.S. (1978). "Wave-induced pore pressure in relation to ocean floor stability of cohesionless soils". Marine Geotechnology 3(2), pp123–150.

Shepherd, R.G. (1989). "Correlations of permeability and grain-size". Ground Water 27(5), pp633-638.

Sumer, B.M., Fredsoe, J., Christensen, S. and Lind, M.T. (1999). "Sinking/floatation of pipelines and other objects in liquefied soil under waves". Coast. Eng. 38(2), pp53-90.

Sumer, B.M., Hatipoglu, F., Fredsøe, J. and Sumer, S.K. (2006). "The sequence of sediment behaviour during wave-induced liquefaction". Sedimentology 53, pp611–629.

Tzang, S.Y. (1998). "Unfluidized soil responses of a silty seabed to monochromatic waves". Coastal Engineering 35, pp283–301.

Yamamoto, T., Koning, H.L., Sellmejjer, H. and Hijum, E. (1978). "On the response of a poro-elastic bed to water waves". Journal of Fluid Mechanics 87 (1), pp193–206.

Zhang, Y., Jeng, D.S., Gao, F.P., Zhang, J.S. (2013). "An analytical solution for response of a porous seabed to combined wave and current loading". Ocean Engineering 57, pp240–247.